Systematic calculation of α decay within a generalized density-dependent cluster model

Dongdong Ni[1,2,*] and Zhongzhou Ren[1,2,3,†]

[1]*Department of Physics, Nanjing University, Nanjing 210093, People's Republic of China*

[2]*Kavli Institute for Theoretical Physics China, Beijing 100190, People's Republic of China*

[3]*Center of Theoretical Nuclear Physics, National Laborator of Heavy-Ion Accelerator, Lanzhou 730000, People's Republic of China*

(Received 31 December 2009; revised manuscript received 21 January 2010; published 17 February 2010)

We perform an extensive investigation on α decays in both even-A and odd-A nuclei within the new version of the generalized density-dependent cluster model. The microscopic deformed potential is numerically constructed in the double-folding model by the multipole expansion method. The coupled-channel effect resulting from nuclear deformation is included by using the coupled-channel Schrödinger equation with outgoing wave boundary conditions. The fine structure observed in α decay is well described by taking into account the angular momentum of the emitted α particle and the Boltzmann distribution of excitation spectrum in daughter nuclei. A good agreement between experiment and theory is achieved, and the results of our calculations are discussed in detail, together with the sensitivity of the calculated half-lives and branching ratios to some physical quantities used in the calculations.

DOI: 10.1103/PhysRevC.81.024315 PACS number(s): 23.60.+e, 21.10.Tg, 21.60.Gx

I. INTRODUCTION

α decay is one of the most important decay channels of unstable nuclei. It has been extensively studied both experimentally and theoretically. Experimentally, α decay has long been a powerful and very precise tool to observe exotic nuclei and investigate their detailed structure [1,2]. In some cases measurements of α decay provide unique information on masses (via the decay energy Q_α) and excitation energies of the closely spaced excited and ground states, for which other common experimental methods are not yet possible. α decay also presents a useful tool to study the spectroscopy of unstable nuclei, which is essentially connected with the phenomenon of α-cluster formation in decaying nuclei [3,4]. In recent experiments, observation of α-decay chains from unknown parent nuclei to known nuclei has been used as a reliable way to identify isomeric states and new synthesized superheavy elements, which is one of the most exciting subjects in contemporary nuclear physics [5–9].

As a large number of α-decay data have accumulated since the very beginning of nuclear physics, a lot of theoretical calculations have been performed to provide realistic interpretation of these data. α decay was described in 1928 as a quantum mechanical tunneling effect [10,11]. This was the first successful application of quantum mechanics to a problem of nuclear physics. More strikingly, it proved the validity of quantum mechanics for nuclei in the late 1920s. Usually, the decay process can be divided into two distinct parts: the formation of an α particle at the nuclear surface, followed by its tunneling through the α-daughter potential barrier. Computing the α-formation amplitude is a difficult task because the actual wave functions involved cannot be well defined. Despite this, progress has been made in two ways: the shell model including Bardeen-Cooper-Schriefer (BCS) pairing [12] and the hybrid model supplementing the shell-model wave function with an α-cluster component [13]. In recent studies, considering that the absolute α-decay width is mainly determined by the product of the α-preformation factor and the barrier penetration probability within the Gamow model, the preformation factor is extracted by dividing the experimental α-decay width by the barrier penetration probability, which can easily be obtained from the Wentzel-Kramers-Brillouin (WKB) approximation [14]. Whatever the formation mechanism, the decay mainly proceeds by a quantum tunneling through the potential barrier. If this barrier is assumed to be spherical, there will be no mixing of orbital angular momentum during the tunneling, and the α-decay width can be evaluated in many entirely different approaches, based on various theoretical models such as the shell model, the fissionlike model, and the cluster model [15–23]. The simple empirical relations between α-decay half-lives and decay energies are also discussed [24–26]. In these calculations, α decay has traditionally been reduced to a one-dimensional semiclassical problem, and all the calculations show similarly good agreement with the experimental data. In fact, a better description of α decay can be achieved if one takes into account the deformed barrier. Indeed, the observation of fine structure in α decay has often been attributed to the tunneling of the α particle through a deformed barrier. A complete explanation of the α-decay process should be able to describe the effect of core deformation. Such effects have been considered in the fusion of heavy nuclei (i.e., the inverse of the quantum tunneling). In this case, some semiclassical methods have been extended to deformed α emitters for a quantitative description of α-decay half-lives, such as the unified model for α decay and α capture [27] and the density-dependent cluster model [28]. However, considering that α decay is fundamentally a typical three-dimensional quantum tunneling effect, these methods turn out to pose some difficulty for a microscopic understanding of α decay. In view of this fact, it is of the utmost importance to develop an exact quantum mechanics approach and characterize the α decay from deformed nuclei.

*dongdongnick@gmail.com

†zren@nju.edu.cn

Recently, we have proposed the generalized density-dependent cluster model (GDDCM) to evaluate α-decay half-lives and its validity has been tested for a wide range of nuclei including the exotic nuclei around the $N = 126$ closed shell [29,30]. As most α-decay studies, we started our microscopic investigation by assuming spherical shapes of both parent and daughter nuclei. Then we further develop the model by taking into account nuclear deformation to fine-tune the theoretical description of α decay. A very recent study on even-even nuclei has already been reported as a Rapid Communication [31]. The purpose of this article is to present detailed formulas of the deformed GDDCM and comprehensive calculations for deformed α emitters including odd-A and odd-odd ones. To our knowledge, this is the first coupled-channel calculation of α decays occurring in odd-A and odd-odd nuclei. In our deformed GDDCM, the parent nucleus is described by an α particle moving in a microscopic deformed potential, which is numerically constructed in the well-established double-folding model by the multipole expansion method. Instead of working in the framework of the semiclassical WKB method along with the Bohr-Sommerfeld quantization condition, the coupled-channel Schrödinger equation with outgoing wave boundary conditions is employed to reproduce the available experimental data concerning α-decay half-lives and branching ratios. The eigencharacteristics of different channels are defined by the Wildermuth condition [32], which severs as a link to the shell model and accounts for the Pauli exclusion principle. From the microscopic viewpoint, our model gives not only a straightforward α-decay calculation but also a quite realistic description of α decay.

This article is organized as follows. In Sec. II, we present the detailed formulas of the calculation of α-decay half-lives within the framework of the deformed GDDCM, and the α-nucleus potential connected with the deformation and orientation is discussed in detail. In Sec. III, the dependence of our calculations on model parameters is discussed in detail, and the theoretical results of our calculations are compared with the experimental data. A summary is given in Sec. IV.

II. GENERALIZED DENSITY-DEPENDENT CLUSTER MODEL

The analysis of α decay can conveniently be made in the framework of the cluster model, which has been shown by the success of extreme cluster models representing the parent state by a pure cluster configuration in describing α decay [33]. The picture we consider here is that of a deformed system, consisting of a spherical α cluster coupled to an axial-symmetric core nucleus with quadrupole and hexadecapole deformations. For such a system, the daughter nucleus violating spherical symmetry generates deformed nuclear and Coulomb potentials, leading to the coupled effect of different channels. And thus a coupled-channel calculation becomes necessary for α decay. The α-core Hamiltonian can be written as

$$H = -\frac{\hbar^2}{2\mu}\nabla^2_{\mathbf{r}} + H_d(\Omega_d) + V(\mathbf{r}, \Omega_d), \tag{1}$$

where μ is the reduced mass of the system, $H_d(\Omega_d)$ is the intrinsic Hamiltonian of the daughter nucleus, describing the rotation of the core with excitation energies E_{J_d}, and $V(\mathbf{r}, \Omega_d)$ represents the interaction between the center of mass of the core and the α particle. The principal dynamical variables in this model are, respectively, the α-core relative coordinate vector $\mathbf{r}$ and the orientation Ω_d of the daughter intrinsic axis with respect to the laboratory reference system.

We proceed by expanding the wave function of the α cluster in a quasibound state into a sum of partial waves with angular and radial components [31,34,35],

$$\Psi(\mathbf{r}, \Omega_d) = \frac{1}{r}\sum_{\alpha} u_\alpha(r)\Theta_\alpha(\Omega, \Omega_d), \tag{2}$$

where $\alpha \equiv (n\ell j)$ completely denotes the channel quantum number, and $u_\alpha(r)$ is the cluster radial function describing the α-daughter relative motion. The angular part is written as

$$\Theta_\alpha(\Omega, \Omega_d) = [Y_\alpha(\Omega) \otimes Y_\alpha(\Omega_d)]_{00}, \tag{3}$$

where $Y_\alpha(\Omega)$ is the orbital-spin wave function of the α cluster, and $Y_\alpha(\Omega_d)$ is the wave function of the daughter nucleus, satisfying the following expression:

$$H_d Y_\alpha(\Omega_d) = E_\alpha Y_\alpha(\Omega_d). \tag{4}$$

We then insert Eq. (2) into the Schrödinger equation $H\Psi(\mathbf{r}, \Omega_d) = E\Psi(\mathbf{r}, \Omega_d)$ and project this equation onto the channel states. After integrating over all coordinates except the radial variable r, we obtain a set of coupled-channel equations for the radial components [31,34,35],

$$\left[-\frac{\hbar^2}{2\mu}\left(\frac{d^2}{dr^2} - \frac{\ell_\alpha(\ell_\alpha+1)}{r^2}\right) - Q_{J_d}\right]u_\alpha(r) + \sum_J V_{\alpha,\alpha'}(r)u_{\alpha'}(r) = 0. \tag{5}$$

In this equation, Q_{J_d}, given by $Q_{J_d} = Q_0 - E_{J_d}$, is the emitted energy of the channel ℓj leaving the daughter nucleus in the state J_d, where Q_0 is the Q_α value for the decay to the ground state. The interaction matrix that contains all of nuclear physics is given by

$$V_{\alpha,\alpha'}(r) = (\Theta_\alpha(\Omega, \Omega_d)||V(\mathbf{r}, \Omega_d)||\Theta_{\alpha'}(\Omega, \Omega_d)), \tag{6}$$

where the parentheses denote integration over all coordinates, save the radial variable r.

To manipulate the dynamics of the coupled system, the main focus lies on the interaction matrix elements consisting of nuclear and Coulomb components. The interaction potential between the center of mass of the core and the α cluster is obtained using the double-folding integral of the realistic nucleon-nucleon (NN) interaction with the density distributions of the α particle and the core nucleus [36,37], that is,

$$V(\mathbf{r}, \Omega_d) = \lambda \int d\mathbf{r_1} d\mathbf{r_2} \rho_1(\mathbf{r_1}) \upsilon(\mathbf{s}) \rho_2(\mathbf{r_2}), \tag{7}$$

where λ is the renormalized factor and $\upsilon(\mathbf{s} = |\mathbf{r} + \mathbf{r_2} - \mathbf{r_1})$ is the effective NN interaction. The spherical density distribution of the α particle $\rho_1(\mathbf{r_1})$ is taken as a standard Gaussian form [38]. The deformed density distribution of the core nucleus

$\rho_2(\mathbf{r_2})$ has the form

$$\rho_2(r_2,\theta)=\frac{\rho_0}{1+e^{[r-R(\theta)]/a}}, \tag{8}$$

where the half-density radius $R(\theta)$ is parametrized as $R(\theta)=R_0[1+\beta_2 Y_{20}(\theta)+\beta_4 Y_{40}(\theta)]$. One of the most widely used effective NN interactions is the popular M3Y interaction based on the G-matrix elements of the Reid potential. Its parameterized form, introduced by Satchler and Love, is given as [38]

$$\upsilon(\mathbf{s})=7999\frac{\exp(-4s)}{4s}-2134\frac{\exp(-2.5s)}{2.5s}+J_{00}(E_\alpha)\delta(\mathbf{s}), \tag{9}$$

and the zero-range pseudopotential $J_{00}(E_\alpha)$, representing the single-nucleon exchange term, is given by

$$J_{00}(E_\alpha)=-276[1-(0.005E_\alpha/A_\alpha)], \tag{10}$$

where E_α and A_α are the kinetic energy and the mass number of the α particle, respectively. For the case of α decay, the energy dependence of the single-nucleon exchange term $J_{00}(E_\alpha)$ is not much in evidence because the α-particle energy E_α generally ranges from 2 to 12 MeV.

In view of the deformed density distribution in the six-dimensional integral, it is a difficult undertaking to derive the microscopic α-nucleus potential. In this case, one usually simplifies the double-folding model by expanding the density distribution of the deformed nuclei using a multipole expansion. In the multipole expansion, the density distribution of the axial-symmetric daughter nucleus is expanded as [39]

$$\rho_2(r_2,\theta)=\sum_{\ell=\text{even}}\rho_2^\ell(r_2)Y_{\ell 0}(\theta). \tag{11}$$

Only even values of ℓ appear in the summation owing to the axial symmetry, and the sum is usually truncated at $\ell=4$. Then the double-folding potential can be evaluated as the sum of different multipole components [39],

$$V(\mathbf{r},\Omega_d)=\sum_{\ell=0,2,4\ldots}V^\ell(r)\Theta_\ell(\Omega,\Omega_d), \tag{12}$$

and the multipole component can be written as

$$V^\ell(r)=\frac{2}{\pi}\int_0^\infty dk k^2 j_\ell(kr)\tilde{\rho}_1(k)\tilde{\rho}_2^\ell(k)\tilde{\upsilon}(k), \tag{13}$$

where the quantity

$$\tilde{\rho}_2^\ell(k)=\int_0^\infty dr r^2\rho_2^\ell(r)j_\ell(kr) \tag{14}$$

is the intrinsic form factor associated with the expanded density distribution $\rho_2^\ell(r)$ of the daughter nucleus, $\tilde{\rho}_1(k)$ is the Fourier transformation of the density distribution $\rho_1(r)$ of the α particle, and $\tilde{\upsilon}(k)$ is the Fourier transformation of the effective M3Y NN interaction. As one can see, the α-nucleus potential is intimately connected with nucleon density distributions in the double-folding model. By relating the density distribution of daughter nuclei to deformation parameters β_2, β_4 and orientation angle θ, the microscopic deformation- and orientation-dependent α-nucleus potential is numerically constructed. As the interaction is expressed in multipoles, the manipulation of the interaction matrix presents no further problem. The matrix elements can then be written in terms of the Clebsch-Gordan coefficient as follows [31,34,35]:

$$V_{\alpha,\alpha'}(r)=\sum_{\ell=0,2,4\ldots}V^\ell(r)\sqrt{\frac{(2\ell+1)(2\alpha+1)}{4\pi(2\alpha'+1)}}\times(\langle\alpha,0,\ell,0|\alpha',0\rangle)^2. \tag{15}$$

The coupled Eq. (5) are solved with boundary conditions. First, the channel wave functions are regular at the origin, $u_{n\ell j}(r\to 0)=0$. Second, in the asymptotic region the nuclear potential vanishes and the Coulomb potential is spherically symmetric. At this point the coupled-channel equations decouple, and the channel wave functions behave as an outgoing Coulomb wave,

$$u_{n\ell j}(r)=N_{\ell j}[G_\ell(k_{J_d}r)+iF_\ell(k_{J_d}r)], \tag{16}$$

where $N_{\ell j}$ are normalization constants, and $G_\ell(k_{J_d}r)$ and $F_\ell(k_{J_d}r)$ are, respectively, the irregular and regular Coulomb wave functions with $k_{J_d}=\sqrt{2\mu Q_{J_d}}/\hbar$. By calculating the decay probability flux through a spherical surface with the asymptotical behavior of the radial wave function, one can ultimately express the partial width of the channel ℓj in terms of the normalization constant,

$$\Gamma_{\ell j}=\frac{\hbar^2 k_{J_d}}{\mu}|N_{\ell j}|^2. \tag{17}$$

The normalization constants $N_{\ell j}$ are obtained by matching each channel wave function $u_{n\ell j}(r)$ to the outgoing Coulomb wave at a large distance R. Then, for a given channel ℓj, the partial decay width corresponding to the decay into a core state J_d is given by

$$\Gamma_{\ell j}(R)=\frac{\hbar^2 k_{J_d}}{\mu}\frac{|u_{n\ell j}(R)|^2}{G_\ell(k_{J_d}R)^2+F_\ell(k_{J_d}R)^2}. \tag{18}$$

Note that the expression of Eq. (18) is valid only for distances beyond the range of the nuclear potential and independent of R. This provides a stringent test of the reliability of the exact formalism presented here. If $\Gamma_{\ell j}(R)$ has a clear dependence on R, then the theory is incorrect. In addition, considering that the α-decay width associated with the imaginary part is usually extremely small, one could as well use the real wave function $G_\ell(k_{J_d}r)$ as an outgoing Coulomb wave, as shown in Refs. [30,31], and [40].

Because the decay energy cannot be predicted with sufficient accuracy for a given potential, as before, we adjust the renormalized factor λ to make all channels simultaneously reproduce the experimental Q_{J_d} values. This means that the α-nucleus potential remains the same for all channels of a given α emitter. Then the main requirements of the Pauli exclusion principle are satisfied by choosing the quantum number n (i.e., the number of internal nodes in the radial wave function) to follow the Wildermuth condition [32],

$$G=2n+\ell=\sum_{i=1}^4 g_i. \tag{19}$$

In this expression, g_i are the corresponding oscillator quantum numbers of the constituent nucleons in the α cluster, whose

values are chosen to guarantee the α cluster entirely outside of the shell occupied by the core nucleus. In the present study, the global quantum number G is taken as follows:

$$\begin{aligned} G &= 18 \quad \text{for} \quad 50 < N \leqslant 82, \\ G &= 20 \quad \text{for} \quad 82 < N \leqslant 126, \\ G &= 22 \quad \text{for} \quad N > 126, \end{aligned}$$

where N is the neutron number of the parent nucleus. This coincides with the previous α-decay studies adopting various interaction potentials [16,19,20].

The total width representing the tunneling through the deformed barrier is a sum of partial channel widths,

$$\Gamma(R) = \sum_{\{\ell j\}} \Gamma_{\ell j}(R), \tag{20}$$

where $\Gamma_{\ell j}(R)$ corresponding to the decay into a core state J_d is given by Eq. (18). Meanwhile, it is convenient to perform a straightforward calculation of branching ratios for α transitions to a core state J_d, which are written as

$$b_{J_d} = \Gamma_{\ell j}(R)/\,\Gamma(R) \times 100\%. \tag{21}$$

To gain a better insight into fine structure in α decay, following Refs. [34] and [35], in the present analysis we define the quantity

$$I_{\ell j} = \log_{10} \frac{\Gamma_{00}}{\Gamma_{\ell j}}, \tag{22}$$

which represents the relative intensity of different channels with respect to the favored channel. In all of these derivations it is assumed that the deformation of the daughter nucleus remains the same as in the decaying nucleus.

The α-decay width can be fairly well reproduced when we use the experimental Q_α values. There are, however, still differences between calculations and experiments. These discrepancies should be improved by the evaluation of the α-preformation factor P_α, which represents the degree of the overlap between the α-cluster plus daughter state and the parent α emitter. From the theoretical point of view, one can in principle evaluate the P_α values from the overlap between the actual wave function of the parent nucleus and the decaying-state wave function describing one α cluster coupled to the residual daughter nucleus. As mentioned in the Introduction, various microscopic calculations of complexity have been concentrated on this issue [12,13]. The nucleus ^{212}Po, as a typical nucleus with two protons and two neutrons outside the double closed shell, has been widely investigated. The representative example is that of Varga *et al.*, in which the weight of α clustering is found to be as high as 0.3 [13]. However, it is extremely difficult to perform further calculations for nuclei including more nucleons outside the double-magic core. The reason is that even a very large shell-model basis is often insufficient to describe the actual situation of α-cluster formation because this process is strongly potential dependent, with the additional complication of the nuclear many-body problem. Experimentally, it is known from the available cases that the preformation factor varies smoothly in the open-shell region and has a value less than unity [41]. With this in mind, a convenient way of performing an analysis of the α-preformation factors is by taking the same preformation factor for a certain kind of nuclei (even-even, odd-A, and odd-odd), which keeps the number of free parameters in the model to a minimum. This is consistent with Buck's model [16]. Nevertheless, there is no doubt that the experimental half-lives should be better reproduced if the preformation factor is considered to vary with different parent nuclei instead of a constant, especially for the closed-shell-region nuclei. This is worth further investigation.

III. NUMERICAL RESULTS AND DISCUSSION

A. Model parameters used in calculations

Because α decay is understood as a two-body phenomenon involving a core nucleus and an α particle, a reliable input of the α-nucleus interaction potential is required for the quantitative description of α decay. In our GDDCM, the α-nucleus potential with a clear dependence on deformations and orientations is numerically constructed in the double-folding model using model parameters, such as the radius and the diffuseness. In the spherical case, the radius and the diffuseness of the density distribution of the core nucleus are taken as $R_0 = 1.07$ fm and $a = 0.50$ fm; this parametrization turns out to work very well in the description of spherical α emitters [29,30]. As a further extension toward deformed systems, we assume that the α-nucleus potential should be the same for the core nucleus in its ground or excited state so that it is not necessary to introduce other new parameters, which would reduce the predictive power of the calculation. Unfortunately, it is found that the preceding parameter set has too small a radius to give a quantitative description of the tunneling rate. This is very similar to the situation of proton emission, where the Becchetti-Greenlees Woods-Saxon parameter set is excellent for spherical proton emitters but performs rather poorly for deformed ones, for the same reason [42]. With this in mind, as in the case of proton emission, a new parameter set, which has slightly larger radii, is taken for deformed α emitters as follows: $R_0 = 1.15$ fm and $a = 0.50$ fm.

As already mentioned, it is indispensable to evaluate the α-preformation factor for absolute α-decay half-lives, and the analysis of the preformation factor P_α can conveniently be made by taking the same preformation factor for one certain kind of nuclei. In combination with the previous spherical calculation, we obtain the preformation factors as follows: $P_\alpha = 0.39$ for even-even nuclei, $P_\alpha = 0.25$ for odd-A nuclei, and $P_\alpha = 0.15$ for odd-odd nuclei. These values agree well with both the microscopic calculations [13] and the experimental results [41]. Furthermore, to well describe fine structure in α decay, we introduce the Boltzmann distribution for excitation spectrum in the daughter nuclei [43],

$$\rho(E_{J_d}) = \exp(-cE_{J_d}), \tag{23}$$

where E_{J_d} (in MeV) is the excitation energy of the daughter state J_d. This may be not so surprising because, as early as 1917, Einstein had proposed this fundamental hypothesis on the quantum theory of radiation, that is, canonical distribution of states [44]. This procedure is also equivalent to the

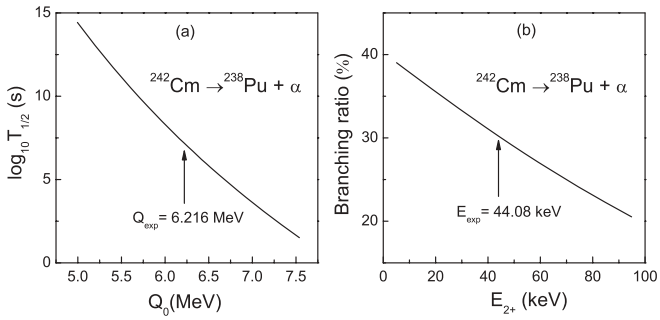

FIG. 1. Sensitivity of the calculated half-life and branching ratio to some physical quantities used in calculations for the α emitter ^{242}Cm. (a) Calculated half-lives as a function of the decay Q_0 value. (b) Calculated branching ratios to the daughter 2^+ state as a function of the excitation energy E_{2^+}. Experimental values of Q_0 and E_{2^+} are indicated.

α-preformation factor with an exponential dependence on the excitation energy of the daughter nucleus. In Ref. [26], such a dependence is clearly evident for the reduced width to excited states. In this way, we obtain a set of parameters for the Boltzmann distribution as follows: $c = 2.3$ for even-even nuclei, $c = 26.3$ for odd-A nuclei, and $c = 28.1$ for odd-odd nuclei.

As we all know, the decay Q_0 value has a crucial effect on the α-decay half-life. To see this strong effect, we have calculated the α-decay half-lives of ^{242}Cm for various Q_0 values. Figure 1(a) illustrates the variation of the calculated half-life as the function of the decay Q_0 value. As the Q_0 value changes from 5.0 to 7.5 MeV, the calculated half-life decreases rapidly by about 13 orders of magnitude, from 10^{14} to 10^1 s. Also, a change in the Q_0 value affects fine structure in α decay, but this effect is much smaller. Very minor changes in branching ratios are found as a function of the Q_0 value.

On the contrary, the strong dependence of the branching ratio on the excitation energy of daughter states is evident in our calculations. For concreteness, in Fig. 1(b) we present the calculated branching ratio to the 2^+ state as the function of the E_{2^+} value for the α-decaying 0^+ state in ^{242}Cm. As the E_{2^+} value is changed from 5 to 95 keV, the branching ratio decreases by about 50% from its original value of 39. Such a change in the E_{2^+} value also has an influence on the calculated α-decay half-life, leading to an increase in the half-life by about 30%. This variation of the half-life is very small because the allowed deviation of calculated half-lives is 200% or 300% in systematic calculations.

B. Systematic results of α decay for different kinds of nuclei

Extensive α emitters, ranging from $Z = 52$ to $Z = 105$, have been systematically investigated within the new version of the GDDCM. The main focus is on well-deformed α emitters exhibiting collective rotational motion. In this case, the different channels are strongly coupled, and the exact solution of the coupled-channel equations, Eq. (5), is indispensable. In contrast, the exact quantum mechanics study of α decay is a simple task in the spherical case, where one needs to deal with only a single radial equation instead of the set, Eq. (5). In our analysis of α decay, the only input data are the mass number A and the charge number Z of the parent nucleus, the deformation β_2 and β_4 parameters of the corresponding daughter nucleus, the decay Q_0 value, and the excitation spectrum in the ground-state band of the daughter nucleus. Among these quantities, as already discussed, the Q_0 value and the excitation spectrum in the daughter nuclei are very crucial in the α-decay study. So their values are set by experiment [45,46]. The deformation parameters of daughter nuclei are taken from Möller *et al.* [47] instead of experiments. The reason for this is that information on the value of hexadecapole deformation is often absent in experiments. Moreover, the values from Möller *et al.* are close to the experimental values of core deformation, and the difference between them has a tiny influence on α-decay calculations. To estimate our theoretical results, the experimental α-decay half-lives are mainly taken from Refs. [46] and [48], and some new data are from Ref. [49].

1. Even-even nuclei

For the case of even-even nuclei, α decay mainly proceeds from ground states 0^+ to ground states 0^+. This means that the angular momentum and parity of the emitted α particle are 0^+. Actually, the even-even parent nuclei can also decay from their ground states to the excited states of the rotational band in the corresponding daughter nuclei, owing to the violation of spherical symmetry. Figure 2 indicates the possible channels that are involved in the α decay of well-deformed even-even nuclei. Considering that the high-spin channels are strongly restrained by the centrifugal barrier, in most cases only the 2^+ level in the daughter nucleus has a profound effect on α-decay calculations, as shown in Fig. 1(b).

A preliminary discussion of our microscopic approach has already been published for even-even nuclei. Here we present only a few typical results of even-even nuclei as a supplement to the previous publication. Before presenting our numerical results, let us discuss the influence of the newly introduced Boltzmann distribution of excited states in the daughter nuclei.

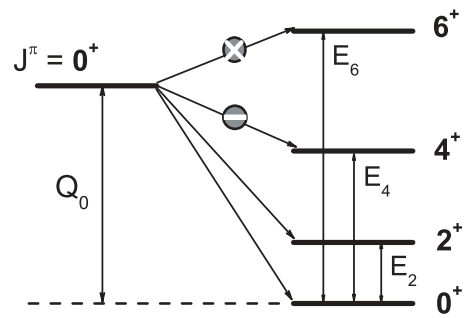

FIG. 2. A survey of the observed α transitions in deformed even-even nuclei. Decay proceeds from the ground state of a parent nucleus to the members of the ground-state rotational band of the corresponding daughter nucleus. Q_0 represents the Q_α value for the transition from ground state to ground state, and E_{J_d} labels the excitation energy of the daughter state J_d with respect to the ground state. Note that the $\ell \geqslant 4$ α transitions are strongly restrained by the large centrifugal barrier.

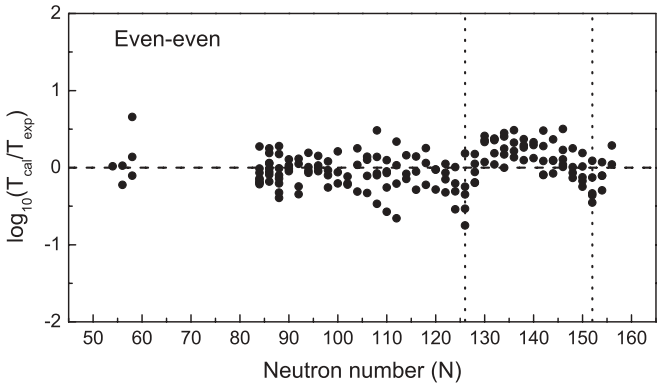

FIG. 3. Deviations of the calculated half-lives from the experimental values versus the neutron number N for even-even nuclei with $Z = 52$–104. The deviations 0.3, 0.4, and 0.5 of the logarithms correspond to the absolute deviations of half-lives by factors of 2.0, 2.5, and 3.2, respectively. Vertical bars indicate spherical and deformed neutron magic numbers of the parent nuclei $N = 126$ and 152.

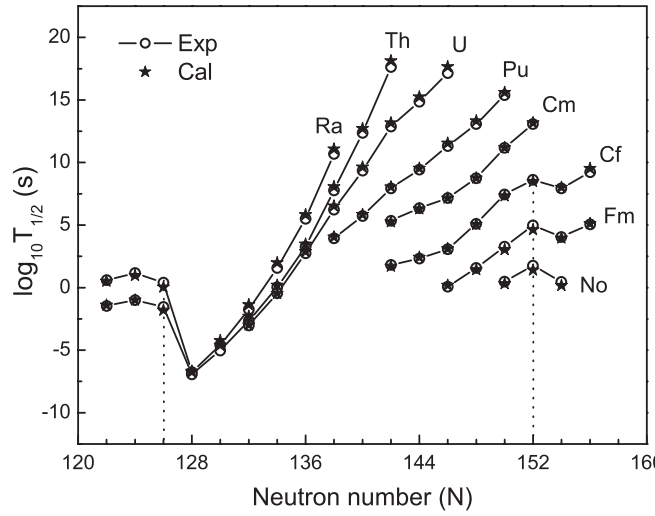

FIG. 4. Comparison of the calculated α-decay half-lives with the experimental data for deformed even-even nuclei ranging from $Z = 88$ to $Z = 102$, showing the strong shell effect at the neutron magic numbers $N = 126$ and 152.

As already shown, the parameter c used in the Boltzmann distribution has a small value for even-even nuclei. This means that the Boltzmann distribution has a small effect on the calculated half-life and branching ratio for even-even nuclei. In general, the half-life is increased by 3%–5%. For the branching ratio to the ground state, the effect is an increase of 1.5%–4.5%. These are not large enough to affect our systematic results for even-even nuclei.

Figure 3 displays the deviations of calculated α-decay half-lives from the experimental data as a function of the neutron number N of the parent nucleus. As one can see, the values of $\log_{10}(T_{\rm cal}/T_{\rm exp})$ are generally within the range of about ± 0.5, which corresponds to the values of the ratio $T_{\rm cal}/T_{\rm exp}$ within the range of about 0.32–3.2. This means that the calculated α-decay half-lives are in good agreement with the experimental data for even-even nuclei. Because the constant preformation factor cannot completely describe the detailed features of nuclear structure, the strong shell effects are clearly shown from the increased deviations in the neighborhood of $N = 126$ and 152. One can also notice that there is another slightly large derivation in Fig. 3, which corresponds to the α emitter ^{194}Pb with the proton magic number $Z = 82$.

Besides the $N = 126$ and 152 shell effects, most even-even superheavy nuclei are characterized by large deformations. It is worth paying special attention to them. The comparison of the calculated α-decay half-lives with the experimental data is illustrated in Fig. 4 for the $Z = 88$–102 isotopes. Circles denote the experimental data, and stars stand for the theoretical results. It is well known that for a given element the decay Q value of isotopes generally decreases with increasing neutron number, resulting in an increase in the half-life. However, in Fig. 4 there is a clear decrease in the half-life before the neutron number $N = 128$, shown in the Ra and Th isotopes. This is attributed to the strong $N = 126$ shell effect: the main effect of the $N = 126$ shell is included in the decay Q value, which is closely related to the nuclear structure, and the remaining effect is largely absorbed into the α-preformation factor. We have performed a detailed investigation of the exotic α decays around the $N = 126$ shell gap [30]. Here we do not repeat it. Similarly, across the $N = 152$ deformed shell, the half-life decreases with increasing neutron number and then increases in the usual way, shown in the Cf, Fm, and No isotopes, but this effect is less significant. Despite the shell effects as well as the large deformations involved, one can see that the theoretical α-decay half-lives follow the experimental ones well over a wide range of magnitude, from 10^{-7} to 10^{18} s.

Before we finish the discussion of the numerical results of even-even nuclei, we would like to add a comment concerning our result on the relative intensity to the 4^+ channel during the α decay of even-even nuclei. When the decay happens to the rotational band of daughter nuclei, the component to the ground state of daughter nuclei is dominant and the next one is the decay to the 2^+ state. The branching ratio to the 4^+ state is low (less than 1%) and we have omitted it in the previous calculations. This is a reasonable approximation for α-decay half-lives. To gain a clear insight into this, we take the data for ^{234}Pu as an example, where the branching ratios of α decay to the 0^+, 2^+, and 4^+ states are 68%, 32%, and 0.4%, respectively [46,49]. We perform numerical calculations within our model by solving three coupled equations, and the numerical results of wave functions are plotted in Fig. 5. Based on the wave functions we obtain the branching ratios 71.1%, 28.6%, and 0.3% for the 0^+, 2^+, and 4^+ states, respectively. A good agreement is reached between experimental data and theoretical results. This is also true for other α emitters. When we further take into account the 4^+ channel, much of the time for numerical computation must be spent on computers and the complexity of the calculations increases greatly. Moreover, there are not many data for the 4^+ state and the error bar for the data is relatively large. Hence, in this article we focus our systematic calculations on the 0^+ and 2^+ states. This is

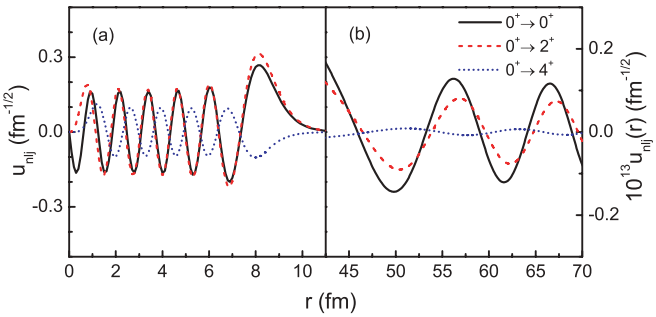

FIG. 5. (Color online) Schematic plot of three-channel wave functions in α decay of the nucleus ^{234}Pu. The solid line (black), the dashed line (red), and the dotted line (blue), respectively, denote the $0^+ \rightarrow 0^+$, $0^+ \rightarrow 2^+$, and $0^+ \rightarrow 4^+$ channel functions. Note that the y axis in (b) is magnified by 10^{13}.

reasonable because the influence of the component to the 4^+ state is marginal for total half-lives. Further research on the relative intensities to more daughter states will be carried out in future.

2. *Odd-A and odd-odd nuclei*

The results of even-even nuclei prove the basic validity of our microscopic approach and give us some confidence in our GDDCM. This stimulates us to make a further investigation of odd-A and odd-odd α emitters. The situation of odd-A and odd-odd nuclei is more complicated than that of even-even nuclei. Their ground-state spin and parity cannot be automatically assigned as those of even-even nuclei. For some odd-A and odd-odd nuclei, information on the ground-state spin and parity is still unavailable in experiments. In addition, their transitions from ground state to ground state usually involve unpaired nucleons, leading to the strong hindrance of the additional centrifugal barrier $\ell \neq 0$. And we have little knowledge of the ℓ value in experiment, except for closed-shell-region nuclei, thanks to only one extra hole/particle outside the closed shell. These are the reasons that the experimental data for even-even nuclei, rather than odd-A or odd-odd nuclei, are usually used as a good test of theoretical models or approaches. And just because of this, we only performed a detailed investigation on even-even nuclei in the previous study [31]. As far as we know, up to now there are few theoretical calculations of α-decay half-lives for odd-A and odd-odd nuclei, especially from the microscopic point. As a further extension of our model toward odd-A and odd-odd nuclei, we base our work on favored α transitions, instead of ground state-to-ground state ones, and take into account the coupled-channel effect as in the case of even-even nuclei. In view of the fact that experimental information is rare for the value of ℓ in the case of odd-A and odd-odd nuclei, we choose the smallest one from the possible ℓ values in our calculations. In fact, for odd-A and odd-odd nuclei their structure effects become very important, and thus they should be adequately investigated for each nucleus rather than globally, in particular, for deformed ones. In the α-decay study of odd-A and odd-odd nuclei, we restrict our attention to the experimentally well-known deformed α emitters.

Table I displays the detailed results of our evaluations for odd-A nuclei. The first column in Table I denotes the parent nucleus. The second and third columns are, respectively, the deformation β_2 and β_4 parameters of the corresponding daughter nucleus. The energy gap of the excitation spectrum in the daughter nucleus is given in column 4. The experimental and theoretical values of the relative intensity given by Eq. (22) are listed in columns 5 and 6. The decay Q value for favored α transition is given in column 7. The experimental and theoretical α-decay half-lives are listed in the last two columns. As one can see, there is reasonable agreement in the relative intensities, and the experimental half-lives are well reproduced within a factor of about 2. In fact, the present analysis of odd-A nuclei is merely preliminary because the actual situation of α transitions in odd-A nuclei may be much more complex than what we expect. On the one hand, both the ℓ values and the experimental branching ratios of many nuclei need to be determined with an improved accuracy. Consequently, the deviations of our results presented in Table I are larger than they should be, especially for the relative intensities. On the other hand, besides the dominant decay channels under investigation, in odd-A nuclei there exist other decay channels resulting from various structure effects, such as channels to the other rotational band in the daughter nucleus and channels with a change in parity. It is interesting and desirable to combine our approach with reliable nuclear structure models to further improve the agreement between experiment and theory. For the sake of a clear insight into the agreement of α-decay half-lives, Fig. 6 shows the comparison of the calculated half-lives with the experimental data for isotopic chains of $Z = 91$–100. We can see that the calculated results follow the experimental data well in the range of 10^{-2} to 10^{16} s. The shell effect at the deformed neutron magic number $N = 152$ is also seen from the isotopic chains of Cf, Es, and Fm.

For the case of odd-odd nuclei, the situation is even more complicated, owing to proton-neutron coupling. Their spins and parities are mostly assigned based on systematics and

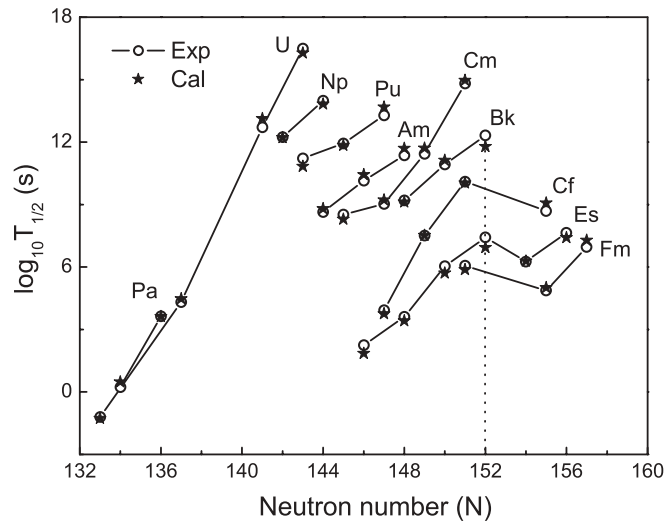

FIG. 6. Same as Fig. 4 except for deformed odd-A nuclei from $Z = 91$ to $Z = 100$. The dotted vertical line stands for the deformed neutron magic number of the parent nuclei, $N = 152$.

TABLE I. Comparison of the calculated α-decay half-lives and relative intensities with the available experimental data for deformed odd-A nuclei involving α-decay fine structure. The α-decay half-life and relative intensity are calculated using Eqs. (20) and (22), combined with the Boltzmann distribution of excited states in daughter nuclei, Eq. (23).

Nucleus	β_2	β_4	ΔE (keV)	$I_2^{\rm exp}$	$I_2^{\rm cal}$	Q (MeV)	$\log_{10} T_{1/2}^{\rm exp}$ (s)	$\log_{10} T_{1/2}^{\rm cal}$ (s)
^{229}Th	0.164	0.112	31.670	0.781	0.733	4.931	11.55	11.85
^{225}Pa	0.111	0.081	52.000	0.368	0.951	7.376	0.23	0.48
^{227}Pa	0.147	0.110	42.400	0.633	0.775	6.573	3.64	3.62
^{225}U	0.102	0.072	47.000	0.689	0.881	8.009	−1.21	−1.27
^{229}U	0.165	0.112	28.000	0.505	0.592	6.473	4.32	4.47
^{233}U	0.190	0.114	42.435	0.805	0.920	4.908	12.71	13.13
^{235}U	0.198	0.115	31.600	0.510	0.775	4.474	16.49	16.28
^{235}Np	0.198	0.115	17.200	0.344	0.470	5.112	12.23	12.22
^{237}Np	0.207	0.117	17.167	0.312	0.477	4.870	13.98	13.83
^{237}Pu	0.207	0.117	33.050	0.552	0.719	5.426	11.22	10.83
^{239}Pu	0.215	0.110	12.964	0.617	0.393	5.244	11.94	11.84
^{241}Pu	0.215	0.102	44.300	0.837	0.968	4.979	13.29	13.69
^{239}Am	0.215	0.110	42.600	0.784	0.850	5.872	8.64	8.81
^{241}Am	0.215	0.102	43.418	0.811	0.903	5.578	10.14	10.44
^{243}Am	0.223	0.095	43.180	0.891	0.920	5.364	11.37	11.70
^{241}Cm	0.215	0.102	12.364	0.581	0.369	6.039	8.51	8.29
^{243}Cm	0.223	0.095	44.664	0.788	0.904	5.882	9.03	9.22
^{245}Cm	0.224	0.079	56.890	1.270	1.171	5.450	11.44	11.71
^{247}Cm	0.224	0.071	51.400	1.179	1.137	4.950	14.81	14.97
^{245}Bk	0.223	0.087	32.638	1.186	0.724	5.984	9.19	9.12
^{247}Bk	0.224	0.071	32.000	0.808	0.733	5.622	10.92	11.13
^{249}Bk	0.224	0.062	28.200	0.670	0.686	5.505	12.32	11.79
^{245}Cf	0.223	0.087	56.100	1.117	1.000	7.256	3.92	3.76
^{247}Cf	0.234	0.073	59.000	1.279	1.125	6.400	7.50	7.52
^{249}Cf	0.234	0.064	54.600	1.244	1.105	5.908	10.11	10.04
^{253}Cf	0.235	0.032	61.242	1.252	1.222	6.076	8.70	9.08
^{245}Es	0.224	0.079	31.000	0.784	0.622	7.858	2.25	1.85
^{247}Es	0.234	0.073	49.000	0.855	0.905	7.444	3.60	3.42
^{249}Es	0.234	0.064	61.000	1.123	1.128	6.887	6.03	5.71
^{251}Es	0.235	0.048	30.000	0.935	0.684	6.597	7.42	6.94
^{253}Es	0.235	0.040	41.790	1.134	0.867	6.739	6.26	6.28
^{255}Es	0.235	0.032	35.100	0.952	1.217	6.503	7.64	7.42
^{251}Fm	0.234	0.057	51.600	1.258	0.991	6.945	6.06	5.87
^{255}Fm	0.236	0.024	59.994	1.268	1.133	7.134	4.87	5.01
^{257}Fm	0.226	0.013	80.200	1.671	1.493	6.623	6.96	7.28

the indirect evidence from α-decay studies. In the large-deformation region, we are only interesting in three odd-odd α emitters, whose spin-parity and α-decay data are well established in experiment. The theoretical results for them are listed in Table II. We can see that, with the Boltzmann distribution of excited states in the daughter nuclei, the α-decay half-lives and relative intensities calculated from the GDDCM agree well with the experimental data. This shows that the GDDCM along with the assumption of Boltzmann distributions has very good accuracy for the α-decay calculations of both odd-A and odd-odd nuclei.

In conclusion, our theoretical results show good agreement with the experimental data for not only even-even nuclei but also odd-A and odd-odd nuclei. The most accurate data are

TABLE II. Same as Table I, but for three deformed odd-odd nuclei, for which experimental spin-parity and decay data are well established.

Nucleus	β_2	β_4	ΔE (keV)	$I_2^{\rm exp}$	$I_2^{\rm cal}$	Q (MeV)	$\log_{10} T_{1/2}^{\rm exp}$ (s)	$\log_{10} T_{1/2}^{\rm cal}$ (s)
^{240}Am	0.215	0.110	42.000	0.859	0.910	5.469	10.99	11.32
^{242}Am	0.215	0.102	65.184	1.201	1.351	5.295	12.01	12.41
^{254}Es	0.235	0.032	70.000	1.554	1.384	6.531	7.40	7.50

those for even-even nuclei. The data for similar transitions in odd-A and odd-odd nuclei are less accurate as a rule, because of the uncertainty of ℓ values, lack of sufficient knowledge of the level schemes in parent and/or daughter nuclei, and other structure effects.

Before ending this article, we would like to mention that there are some other approaches to investigating fine structure in α decay. Recently, a simple barrier penetration approach was proposed to calculate α-decay branching ratios for even-even nuclei [43]. A further calculation of α decays to excited states of even-even nuclei was carried out within the generalized liquid drop model [50]. A study of α decays to ground and excited states was also performed for heavy deformed nuclei in the framework of the unified model for α decay and α capture [51]. All these approaches treated α decay as a one-dimensional problem and worked in the framework of the well-known WKB semiclassical approximation. The experimental branching ratios of α decays to rotational states are well reproduced, and all of them should be considered as an effective theory. Additionally, the coupled-channel approach was also employed to describe α-decay fine structure in even-even nuclei, in combination with a double-folding potential plus a repulsive core [34,35]. In this case, α decay is understood as a three-dimensional quantum problem, instead of a simple one-dimensional one. The cost is that the exact solution of the coupled-channel Schrödinger equation becomes necessary. With this approach, the α-decay fine structure to rotational states is explained with remarkable success. It should be pointed out that our model works in the coupled-channel framework as well but adopts different techniques to deal with the interaction potential and the coupled equations. Despite this, the results of our model agree well with those of Refs. [34] and [35]. This confirms that the coupled-channel approach is very successful in describing α-decay fine structure.

IV. SUMMARY

In summary, we have presented in this paper an extension of the newly developed GDDCM to include odd-A and odd-odd α emitters. In the GDDCM, the microscopic deformed potential is numerically constructed in the double-folding model by the multipole expansion method. The decay width is computed using the coupled-channel Schrödinger equation with outgoing wave boundary conditions. In the case of spherical α emitters, there is a single channel for α decay, and thus one needs to solve only a single radial equation to evaluate the decay width. In the deformed case, where the excited and ground states in daughter nuclei are closely distributed, the different channels are strongly coupled, as one would expect. One must exactly perform coupled-channel calculations for both α-decay half-lives and branching ratios.

The sensitivity of the calculated half-lives and branching ratios to some physical quantities used in the calculations has been discussed. In general, α-decay half-lives have a strong dependence on the decay Q_0 value but depend rather weakly on the excitation spectrum in the daughter nuclei. In contrast, branching ratios show a high sensitivity to the excitation spectrum in the daughter nuclei, while the decay Q_0 value is expected to have little influence on them.

The validity and applicability of the GDDCM have been tested for a wide range of even-even nuclei, and further calculations are performed for deformed odd-A and odd-odd nuclei, which exhibit α transitions similar to those of deformed even-even nuclei. Considering the strong structure effect in odd-A and odd-odd nuclei, we assume that the excitation spectrum in daughter nuclei satisfies the Boltzmann distribution, which is very similar to the hypothesis of Einstein for atomic spectrum. The results reported in Tables I and II are in good agreement with the available experimental data. Despite this, the preset analysis is merely the beginning because the actual situation of odd-A and odd-odd nuclei is more complex than what we consider here. Besides the dominant decay channels under investigation, there exist other channels resulting from various structure effects, such as channels to the other rotational band in the daughter nucleus and channels with a change in parity. We expect the present study of odd-A and odd-odd nuclei to be an important step toward a complete description of them. Efforts toward this objective are being made.

ACKNOWLEDGMENTS

We are thankful to Chang Xu for helpful discussion and comments. This work WAs supported by the National Natural Science Foundation of China (Grant Nos. 10535010, 10675090, 10775068, 10735010, and 10975072), by the 973 National Major State Basic Research and Development of China (Grant No. 2007CB815004), by CAS Knowledge Innovation Project No. KJCX2-SW-N02, and by Research Fund of Doctoral Point (RFDP) Grant No. 20070284016.

[1] R. D. Page *et al.*, Phys. Rev. C **53**, 660 (1996).
[2] A. P. Leppänen *et al.*, Phys. Rev. C **75**, 054307 (2007).
[3] J. Wauters *et al.*, Phys. Rev. Lett. **72**, 1329 (1994).
[4] R.-D. Herzberg, J. Phys. G **30**, R123 (2004).
[5] S. Hofmann and G. Münzenberg, Rev. Mod. Phys. **72**, 733 (2000).
[6] Yu. Ts. Oganessian *et al.*, Phys. Rev. C **74**, 044602 (2006); **72**, 034611 (2005).
[7] T. N. Ginter *et al.*, Phys. Rev. C **67**, 064609 (2003).
[8] K. Morita *et al.*, J. Phys. Soc. Jpn. **76**, 045001 (2007).
[9] A. N. Andreyev *et al.*, Phys. Rev. C **80**, 024302 (2009); **79**, 064320 (2009).
[10] G. Gamow, Z. Phys. **51**, 204 (1928).
[11] E. U. Condon and R. W. Gurney, Nature **122**, 439 (1928).
[12] D. S. Delion, A. Sandulescu, and W. Greiner, Phys. Rev. C **69**, 044318 (2004).
[13] K. Varga, R. G. Lovas, and R. J. Liotta, Phys. Rev. Lett. **69**, 37 (1992).
[14] H. F. Zhang and G. Royer, Phys. Rev. C **77**, 054318 (2008).
[15] S. A. Gurvitz and G. Kalbermann, Phys. Rev. Lett. **59**, 262 (1987).

[16] B. Buck, A. C. Merchant, and S. M. Perez, At. Data Nucl. Data Tables **54**, 53 (1993).
[17] R. G. Lovas, R. J. Liotta, A. Insolia, K. Varga, and D. S. Delion, Phys. Rep. **294**, 265 (1998).
[18] C. Xu and Z. Ren, Nucl. Phys. **A753**, 174 (2005).
[19] P. Mohr, Phys. Rev. C **73**, 031301(R) (2006).
[20] J. C. Pei, F. R. Xu, Z. J. Lin, and E. G. Zhao, Phys. Rev. C **76**, 044326 (2007).
[21] N. G. Kelkar and H. M. Castañeda, Phys. Rev. C **76**, 064605 (2007).
[22] P. R. Chowdhury, C. Samanta, and D. N. Basu, Phys. Rev. C **77**, 044603 (2008).
[23] G. Royer, J. Phys. G **26**, 1149 (2000).
[24] D. N. Poenaru, I. H. Plonski, and W. Greiner, Phys. Rev. C **74**, 014312 (2006).
[25] D. Ni, Z. Ren, T. Dong, and C. Xu, Phys. Rev. C **78**, 044310 (2008).
[26] D. S. Delion, Phys. Rev. C **80**, 024310 (2009).
[27] V. Yu. Denisov and H. Ikezoe, Phys. Rev. C **72**, 064613 (2005).
[28] C. Xu and Z. Ren, Phys. Rev. C **73**, 041301(R) (2006); **74**, 014304 (2006).
[29] D. Ni and Z. Ren, Nucl. Phys. **A825**, 145 (2009); **A828**, 348 (2009).
[30] D. Ni and Z. Ren, Phys. Rev. C **80**, 014314 (2009).
[31] D. Ni and Z. Ren, Phys. Rev. C **80**, 051303(R) (2009).
[32] K. Wildermuth and Y. C. Tang, *A Unified Theory of the Nucleus* (Academic Press, New York, 1997).
[33] B. Buck, A. C. Merchant, and S. M. Perez, Phys. Rev. Lett. **72**, 1326 (1994).
[34] D. S. Delion, S. Peltonen, and J. Suhonen, Phys. Rev. C **73**, 014315 (2006).
[35] S. Peltonen, D. S. Delion, and J. Suhonen, Phys. Rev. C **78**, 034608 (2008).
[36] G. Bertsch, J. Borysowicz, H. Mcmanus, and W. G. Love, Nucl. Phys. **A284**, 399 (1977).
[37] A. M. Kobos, B. A. Brown, P. E. Hodgson, G. R. Satchler, and A. Budzanowski, Nucl. Phys. **A384**, 65 (1982).
[38] G. R. Satchler and W. G. Love, Phys. Rep. **55**, 183 (1979).
[39] M. J. Rhoades-Brown *et al.*, Z. Phys. A **310**, 287 (1983).
[40] C. N. Davids and H. Esbensen, Phys. Rev. C **61**, 054302 (2000).
[41] P. E. Hodgson, and E. Běták, Phys. Rep. **374**, 1 (2003).
[42] A. T. Kruppa, B. Barmore, W. Nazarewicz, and T. Vertse, Phys. Rev. Lett. **84**, 4549 (2000); B. Barmore, A. T. Kruppa, W. Nazarewicz, and T. Vertse, Phys. Rev. C **62**, 054315 (2000).
[43] C. Xu and Z. Ren, Nucl. Phys. **A778**, 1 (2006).
[44] A. Einstein, Phys. Z. **18**, 121 (1917).
[45] G. Audi, A. H. Wapstra, and C. Thibault, Nucl. Phys. **A729**, 337 (2003).
[46] R. B. Firestone, V. S. Shirley, C. M. Baglin, S. Y. Frank Chu, and J. Zipkin, *Table of Isotopes*, 8th ed. (Wiley Intersicence, New York, 1996).
[47] P. Möller, J. R. Nix, W. D. Myers, and W. J. Swiatecki, At. Data Nucl. Data Tables **59**, 185 (1995).
[48] G. Audi, O. Bersillon, J. Blachot, and A. H. Wapstra, Nucl. Phys. **A729**, 3 (2003).
[49] NNDC of the Brookhaven National Laboratory, http://www.nndc.bnl.gov.
[50] Y. Z. Wang, H. F. Zhang, J. M. Dong, and G. Royer, Phys. Rev. C **79**, 014316 (2009).
[51] V. Yu Denisov and A. A. Khudenko, Phys. Rev. C **80**, 034603 (2009).